Journal of the Korean Physical Society, Vol. 76, No. 1, January 2020, pp. 1∼7

Two Local States of Ambient Water

Yongjin Lee*
Department of Physics, Pohang University of Science and Technology, Pohang 37673, Korea

YoungKyu Lee*
Department of Physics and Research Institute of Natural Science, Gyeongsang National University, Jinju 52828, Korea

SeongMin Jeong
IBS Center for Soft and Living Matter, Ulsan National Institute of Science and Technology (UNIST), 50 UNIST-gil, Ulju-gun 44919, Korea

Anupam Kumar
Institute of Chemical Processes, Seoul National University, Seoul 08826, Korea

YongSeok Jho†
Department of Physics and Research Institute of Natural Science, Gyeongsang National University, Jinju 52828, Korea

(Received 1 November 2019; revised 15 November 2019; accepted 20 November 2019)

The non-monotonic trends of thermodynamic response functions have long been a mystery of water. The idea, that water may be a mixture of two local states, came out more than a century ago to explain the origin of the non-monotonic behaviors. Recently, this idea is materialized through the hypothesis of the second critical point of water and then the anomalies are outcomes of critical fluctuation. Although the typical macroscopic heterogeneity (Widom line) of critical fluctuation stays in the vicinity of the critical point, as we have previously shown that the microscopic heterogeneity is identified far from it which extends the linear heterogeneity, the Widom line, to the areal one as a Widom Delta. With this background, we search for two local states of the ambient water. Distinct states in ambient condition are not to be contrasted by a single strong feature such as density but they are expressed by a combination of weak features that reflects locally correlated structures. In this work, we identify the formation of local bicontinuous micro-domain formations of water attributing its softness by using machine learning order parameters. Interestingly, the radial distribution functions are similar to two phases in the liquid-liquid phase transition and they are well fitted by the two-state model. The hard-label domain is dominant at a lower temperature but changes its label to a more fluctuating soft-label domain at high temperature. There exist crossover behaviors around 310–320 K. At sufficiently high temperatures, near the liquid-gas phase transition, all water molecules become homogeneous.

PACS numbers: 05.70.Fh, 64.70.Ja, 47.57.−s
Keywords: Water Anomaly, Liquid-Liquid Phase Separation, Widom Delta, Machine Learning
DOI: 10.3938/jkps.76.1

I. INTRODUCTION

Water is one of the most common liquid on earth and at the same time one of the most special liquids that have more than seventy anomalies. Among them, having its density maximum at 4 °C is its signature anomaly that would have contributed to an origin of life [1–3]. This kind of non-monotonic behavior is also observed in other thermodynamical response functions, too, contrary to the fact that thermodynamical response functions of conventional liquids decrease monotonically on decreasing temperature. For example, the isothermal compressibility increases below 46 °C, isobaric heat capacity is increasing below 35 °C. Also, the thermal expansion coefficient becomes negative below 4 °C, which implies the

*These authors contributed equally to this work.
†E-mail: ysjho@gnu.ac.kr

volume expansion at low temperatures. There have been intensive studies to uncover the secret of water anomalies, but it is not fully understood, yet [4–6]. One interesting hypothesis is that although the global phase of ambient water is a single phase and thus homogeneous, the local structure can be heterogeneous. This idea was further extended to the existence of a first order phase transition of two liquid phases with different densities at very low temperature and high pressure which is so called the liquid-liquid phase transition (LLPT). In this regime, a high density liquid phase of water coexists with a low density liquid phase which would be more structured. However, the possible location of the liquid-liquid critical point (LLCP) is placed in "No man's land" *i.e.* it has not been accessible by the current experimental techniques, and its existence is still controversial [5,7,8].

Although the experimental study is limited, it has been reported that LLCP may exist through numerical simulations [7, 8]. The studies have been extended to beyond the critical point and found that there exists a Widom line (WL) as an extension of the critical point. Along this line, even though the thermodynamical response functions are not divergent anymore, they are locally maximized and macroscopic heterogeneity still can be identified. In this work, the liquid-like state and the gas-like state were trained in the subcritical regime and applied to classify the supercritical fluid. This makes the connection between subcritical phases and supercritical states stronger. Then, can we find the macroscopic heterogeneity in ambient conditions, too? Unfortunately, the Widom line terminates near the critical point. For liquid-gas critical point, it terminates over a 15% higher temperature than the critical point. Beyond this point, the Widom line, the local maxima of individual thermodynamical response functions are split into different lines. Thus, the macroscopic heterogeneity is hard to justify at ambient water condition.

Recently, it has been reported that this reminiscence of phase separation still survives far from the critical point. This can be identified with the microscopic configurations and it agrees very well with the Widom line at the very near to the critical point. This heterogeneity spreads over Widom delta in a form of locally separated states which keeps features of subcritical phases [9]. For this, we have to be able to classify local states, *i.e.* a mixture of two different local states can coexist even in ambient water. According to this idea, ambient water can be interpreted as a mixture of two liquid states and maybe a supercritical state of the LLPT.

The diagnosis of possible coexistence of two local states is not straightforward because the water structure is not firm but very fluctuating. To obtain a reliable correlation of local structure from fluctuating configuration, we examine the kinetic arrestment of water by hydrogen bonds with its neighbors and make their connection to local structures to define the softness of the local water. In other words, we examine the local states involving collective modes from the fluidic state. Throughout this research, we reveal the coexistence of two local states (one is harder and the other is softer) which may be traces of LLPT and the origin of density anomaly.

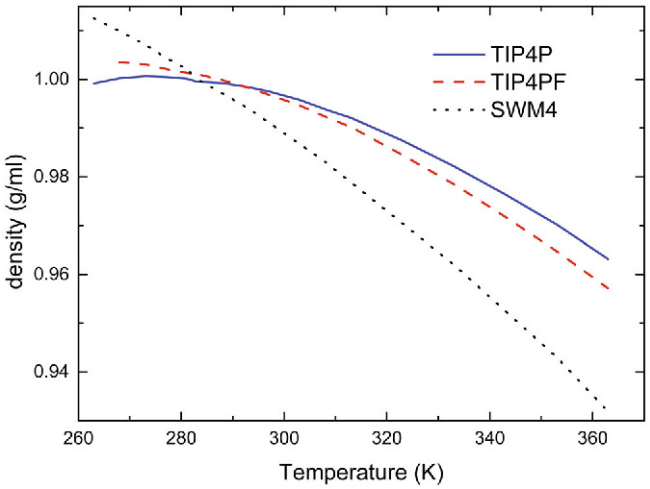

Fig. 1. (Color online) The densities of water as a function of temperature are plotted for the different water models.

II. RESULTS AND DISCUSSION

We have performed the molecular dynamics simulations of ambient water using three classical models, TIP4P/2005 [10], TIP4P/2005f [11], and SWM4-NDP [12](hereafter referred to as TIP4P, TIP4PF, and SWM4 respectively). These models are different in their ways of dealing with the polarization of water which is known to be essential to describe some aspect of water. Here we would like to see whether the polarization effect is essential even in bulk water anomalies. TIP4P is a non-polarizable model, and TIP4PF approximates the polarization effect by considering harmonic spring between covalent bonds. SWM4 introduces the Drude particle to mimic the polarization effect and would reflect the polarization effect most accurately among the three models. Figure 1 shows the variation of density of water according to temperature. The well-known density anomalies are better observed in the non-polarizable model. SWM4 shows monotonic decays in density and doesn't show any non-monotonic behavior within the temperature range we investigated. On the other hand, the oxygen-oxygen radial distribution function agrees better with experiments [13,14] when the water model considers polarizability more carefully (Fig. 2). Unlike the non-polarizable model that may capture the macroscopic behavior better, the microscopic properties seem to be better expressed within the polarizable model [14]. Using these three models, we have studied the transient behaviors at the microscopic level which may be the origin of the macroscopic behavior.

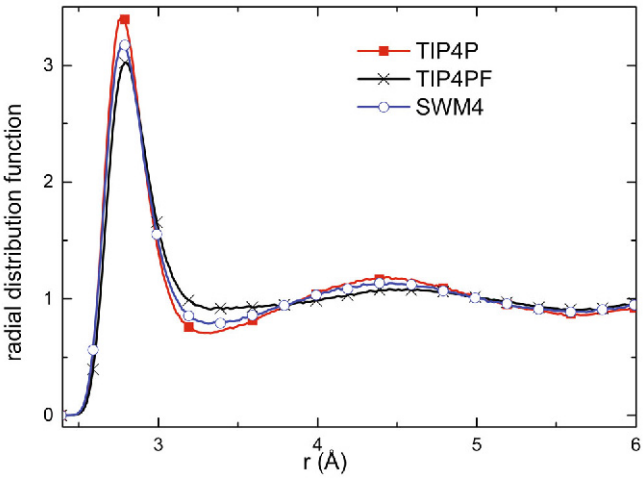

Fig. 2. (Color online) RDFs are presented for the different water models.

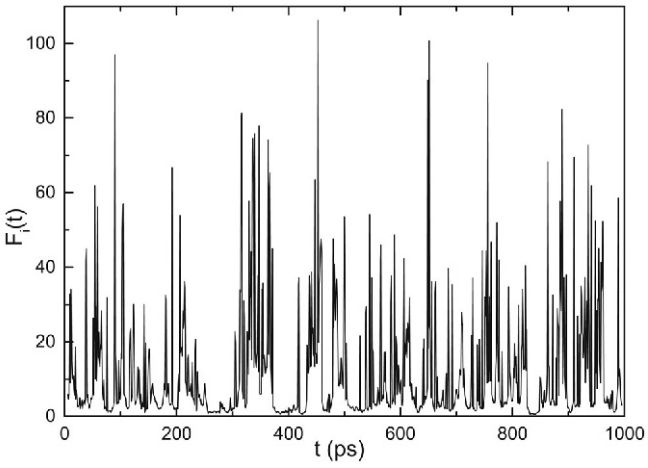

Fig. 3. $F_i(t)$ as a function of time t. The cutoff for soft/hard labelling is set as values between 12–18.

The local structure of ambient water is very delicate to be distinguished in terms of structuredness. Although it is not straightforward to distinguish the local states of the water because its structure is uniform over space on an average, it may be still possible to distinguish the local states based on its kinetic behavior. Recently, Schoenholz *et al.* [15,16] proposed a machine learning way to quantify the local softness of glass. In their approach, the local arrestment of glass particles is meaningfully related to the local structural order parameters. This is consistent with the fact that low-density water (LDL) is glass-like while high-density water (HDL) is fluid-like. In this work, we adopt this idea and classify the local states of water based on the degree of softness. At each time step, we calculate the softness of the particles using the following function,

$$F_i(t) = \sum_{s=-s_0}^{s_0} \prod_{j=1}^{N_{nn}} ||\vec{r}_i(t+s) - \vec{r}_j(t+s)| - r_0| \,, \qquad (1)$$

where r_0 is a distance to the first peak of RDF, and $\vec{r}_j(t)$ is the coordinate of jth nearest neighbors of particle i at time t. We consider a total N_{nn}, the number of nearest neighbors within the cutoff radius which is chosen as the first minimum at the radial distribution functions. As seen in Fig. 3, water molecules vibrate under arrestment for most of its time but jump to other positions suddenly. In other words, the function $F_i(t)$ shows sharp peaks when water molecules are changing their relative positions. Although the transition time itself is very short, the function $F_i(t)$ keeps relatively large values for some time before and after the transient peak. On the other hand, it has small values while the water molecules are arrested by its neighbors. We consider the particles in this transient behavior as soft particles, and the others as hard particles. The criterion for dividing two regimes are a bit arbitrary. We choose the value large enough so that the fluctuation of hard particles are screened. However, it turns out that this criterion is not critical to training. As long as the criterion is large enough, the classification results are very similar.

After the water molecules are labeled as their kinetic properties, we train them with their local structure. If the kinetic properties are from the collective behavior of the system, they would be dependent on the local structures. However, the order parameter of the system is not simple to be expressed by a single order parameter such as density which is a typical order parameter describing the phase transition in simple liquid. Instead, we will use a combination of several parameters that reflects local structures. Three-dimensional bond order parameters (BOP: Q_4, W_4, Q_6, and W_6) [17], Voronoi volume, number of Voronoi neighbor [18], local structure index (LSI) [19] and number of hydrogen bond. The bond order parameters are a set of structural parameters that show "the degree of crystallinity" using relative orientations of a particle with its nearest neighbors. The local structure index (LSI) is another structural parameter associated with the distribution of radial distances of the nearest neighbors of a particle. These parameters are served as order parameters for solid-liquid, liquid-liquid, liquid-gas phase transitions of water.

We make a list of every water molecules in all frames. To make the input set unbiased, we randomize the list, *i.e.* there is no spatial correlation between inputs. So, if there is a correlation in output, it reflects the intrinsic correlation of the system. LIBSVM [20] is used for classification and the training accuracy is about 75%, which proves a robust consistency in classification. Prediction accuracy is over 75%.

In Fig. 4, we plot the configurations of ambient water at different temperatures. Water molecules are shown as single spheres, and colors represent softness of the molecules: red for soft particle and blue for hard particle. It is observed the domain formation of soft water molecules and hard water molecules. This indeed in-

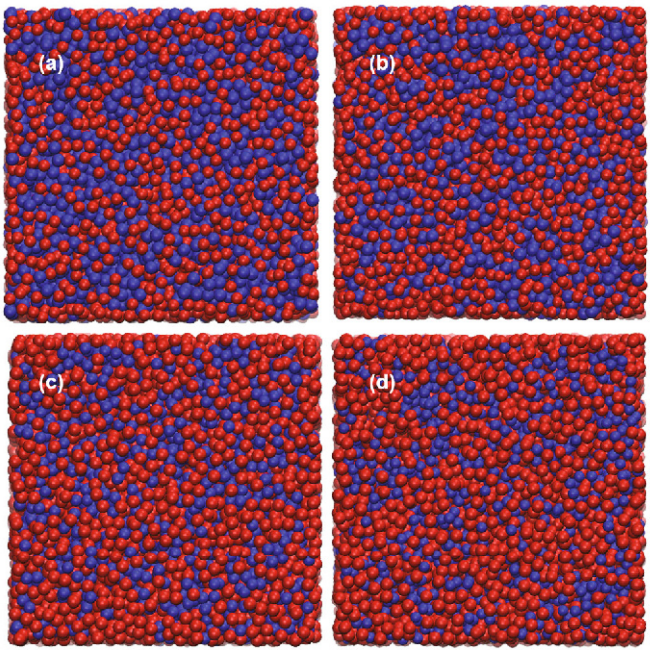

Fig. 4. (Color online) Labeled configurations of ambient water at different temperature. The temperatures are (a) 263 K, (b) 293 K, (c) 323 K, (d) 363 K. Red spheres represent water molecules in the soft state and blue ones correspond to water molecules in the hard state.

dicates that the soft waters are not from the random process but have a physical origin (we would like to remind that we have removed all the spatial correlation by performing online learning.). However, there still could exist mislabeled particles which are surrounded by other labels. To compensate them, we relabel the local states by considering the states of their nearest neighbors using the following formula, $\sigma_i = \left(\frac{1}{N_{nn}} \sum_{j \in nn} \left| s_j^0 - s_i^0 \right| \right)$. Here, i is a particle number, nn is the nearest neighbors, and s_i^0 is the original label of the i^{th} water molecule (0 for Hard and 1 for Soft). In this work, we change the label of i^{th} water molecule (from Hard to Soft or Soft to Hard) if $\sigma_i > x_{th}$ and do not change otherwise. x_{th} is a threshold value which is chosen as 0.8 in this work. Thus, we invert the label of the particle if less than 20% of neighbors have the same label. The number of mislabeled particles is about $1.8\% \pm 0.4\%$.

It is interesting to contrast the physical properties of the two local states. Figure 5 shows the RDFs when the reference particles are soft or hard obtained by using the machine learning technique at temperatures, (a) 263 K and (b) 363 K. Note that the radial distribution function is measured between the labeled reference particle and all the rest particles regardless of their labels. Thus, it would be a simple division of total RDF in Fig. 2 with respect to the label of reference particles. A bit surprisingly, two RDFs are completely different. The RDF of hard particles is very similar to that of LDL. In contrast, the RDF of soft particles is like that of unstructured fluid

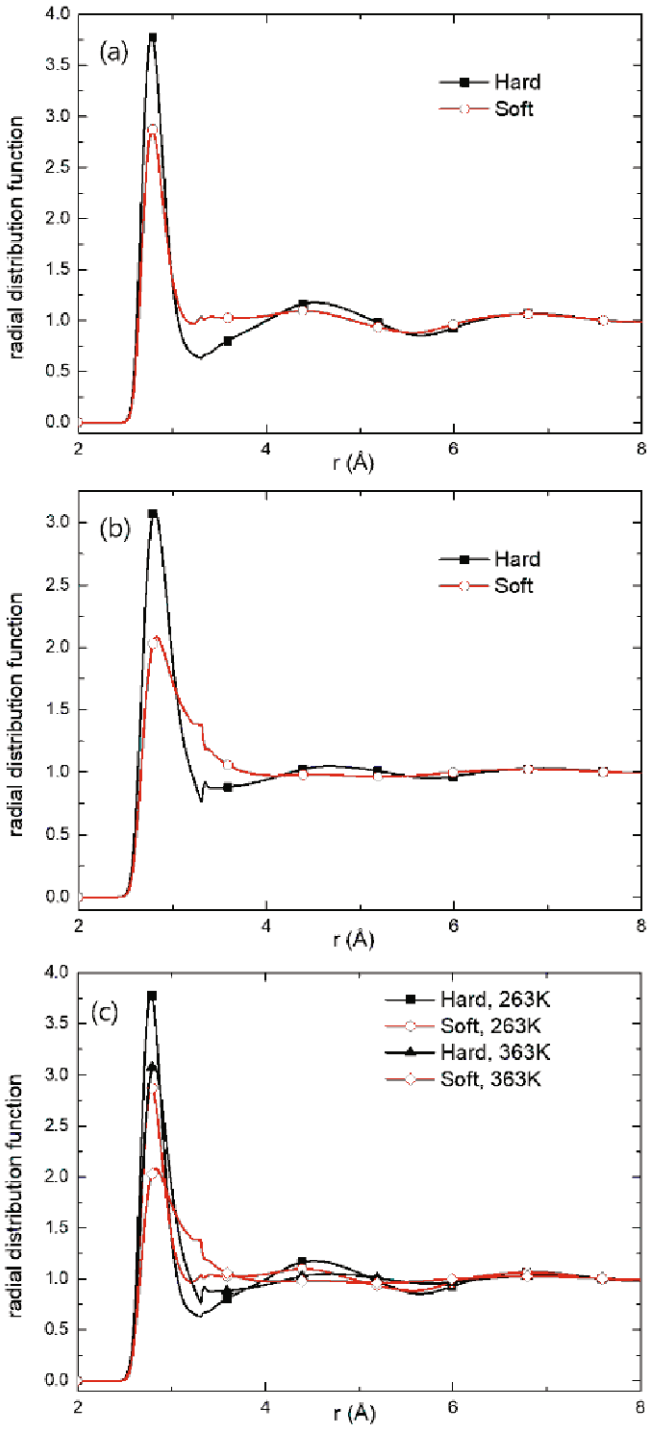

Fig. 5. (Color online) Radial distribution functions g_{SA} and g_{HA} are plotted at temperatures, (a) 263 K and (b) 363 K (c) for both 263 K and 363 K . g_{SA} is the radial distribution function for the pair between the reference particle in the soft state and all the rest water particles. And g_{HA} is the radial distribution function for the pair between the reference particle in the hard state and all the rest water particles.

or HDL [21]. The positions of the first peak of RDFs of both the particles remain fixed at these temperatures.

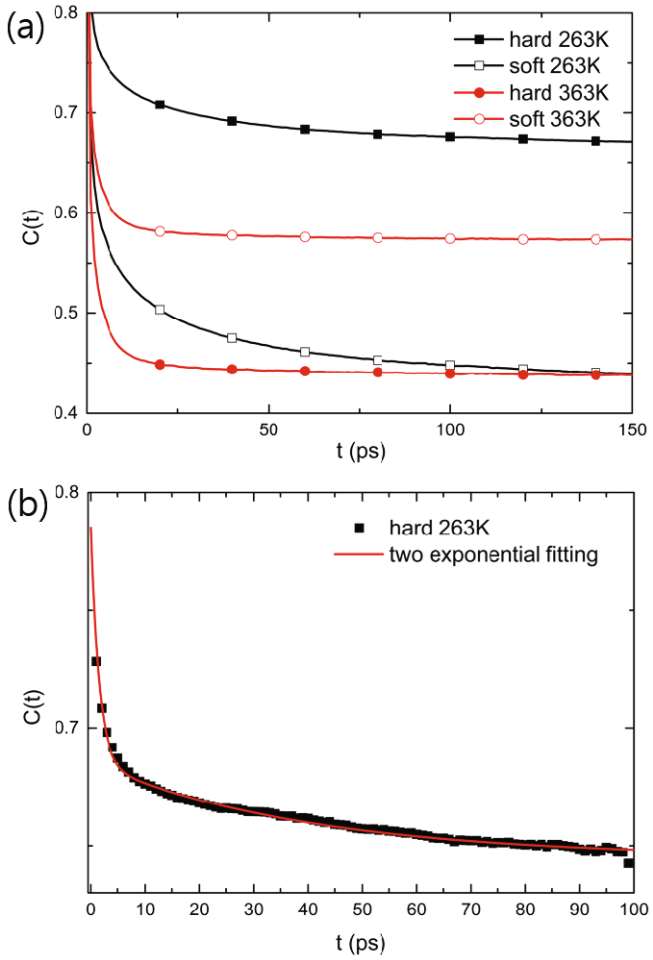

Fig. 6. (Color online) (a) Lifetime of soft and hard states at different temperatures for TIP4P water model. (b) Two exponential fitting of the lifetime of hard labeled water at 263 K. The fitting function is $0.1\exp(-x/1.5) + 0.04\exp(-(x-3)/40) + 0.645$.

The intensity of the RDFs' peak decreases as well as expands in their range with increasing temperature similar to a normal fluid. Although the difference in intensities of the first peak of RDFs of the hard particles and the soft particles remain constant at these temperatures, we observed discontinuity in the first peak of RDFs at a higher temperature value of 363 K. The discontinuity appearing at higher temperatures in both states indicates that their nearest neighbors may consist of particles of mixed states. Unlike this noticeable difference in RDFs, the number of hydrogen bonds is still large enough to be 3.5 or so for both the states. Thus, this regime of water is still entropy dominant. They can readjust themselves to the hydrogen bond network. It is more advantageous to keep a large number of hydrogen bonds although individual bond energy may decrease a little bit. In this way, they can keep the hard state up to high temperature not undergoing phase transition though the number gets less.

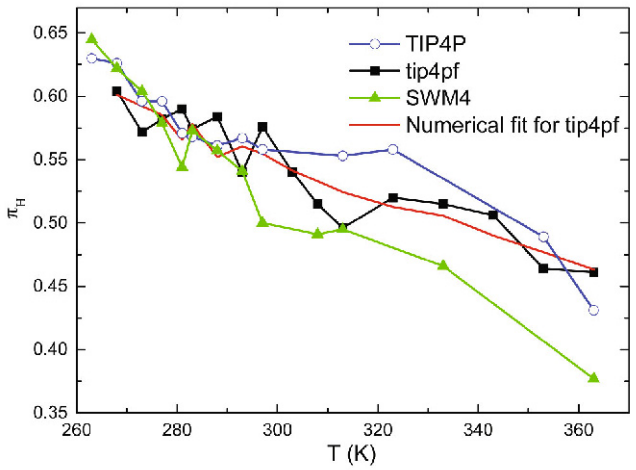

Fig. 7. (Color online) Fraction of the hard states. Filled Squared line plots the results of the numerical simulation and the red line is fitting curve from two-state model in Eq. 4.

Next, we plot the autocorrelation functions of two water labels in Fig. 6.

$$\begin{aligned} C_H(t) &= \langle s_i(0)s_i(t)\rangle, \\ C_S(t) &= \langle (1-s_i(0))\,(1-s_i(t))\rangle, \end{aligned} \quad (2)$$

where H and S denote hard and soft labels. The convergence of the $C(t)$ is dependent on their fraction at each temperature. We fit the autocorrelation functions as two exponential decay functions to obtain two-time scales. The lifetime of the hard state is longer than that of the soft state at low temperatures which turns to be opposite at high temperatures. The short lifetimes are about an order of 1.5 ps to be comparable with the breakage of a hydrogen bond [22]. Although the individual lifetime is short, the relaxation of the local domain, corresponding to a long lifetime, takes much longer depending on the size of the domain. Hence the long time relaxation is larger at low temperatures at which the domain size is thicker. It is about 40 ps for hard domain at 263 K in Fig. 6(b).

Indeed these behaviors are critically dependent on temperature. In Fig. 7, the fraction of the hard state has been presented as a function of temperature. Particles with larger kinetic energy will be easier and simpler to break the hydrogen bond and turns to be soft. The same trend can be observed as a transition lifetime. From the conventional two-state model, the total free energy of the system is described by,

$$G = \pi_{\rm H} G_{\rm H} + \pi_{\rm S} G_{\rm S} + k_{\rm B}T\left[\pi_{\rm H}\ln\pi_{\rm H} + \pi_{\rm S}\ln\pi_{\rm S}\right]. \quad (3)$$

Here, $G_{\rm H}$ and $G_{\rm S}$ are the Gibbs free energies of hard and soft states, respectively. The equilibrium fraction is obtained from the minimization of G,

$$\pi_{\rm H} = \frac{1}{[1+e^{\Delta G}]}, \quad (4)$$

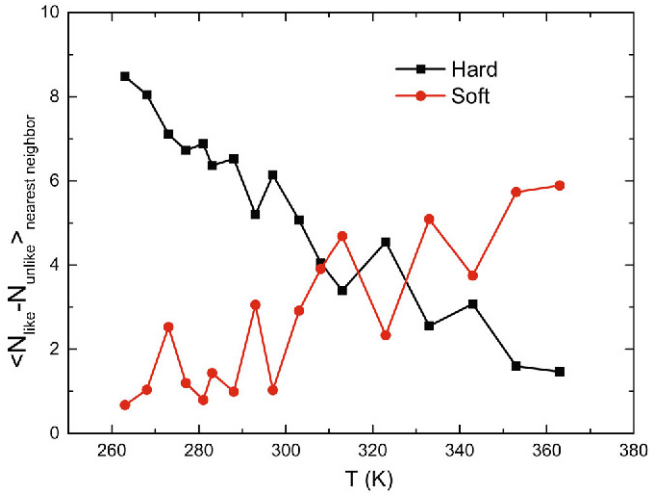

Fig. 8. (Color online) Margin of same label particles and different label particles among Voronoi neighbors is plotted as a function of the temperature. Filled square is when the label of the reference particle is hard and filled circle is when the label of the reference particle is soft.

where $\Delta G = (G_{\rm H} - G_{\rm S})/(k_{\rm B}T)$. The free energy is divided into three terms depending on temperature and volume difference, $\Delta G = U - T\Delta S + P\Delta V$, where U is internal energy, S is an entropy, P is pressure and V volume. T, P and ΔV are obtained from the simulation and the rest are considered as fitting parameters. The simulation results exhibit good agreement with the theoretical fitting of the two-state model.

On increasing the temperature, the first peak of RDFs gets lower while the width of the peak becomes broader. The relaxation of the hydrogen bonded network will be enhanced accordingly. The entropy of the system will also increase while the enthalpy of the system does not change much as in hydrophobic assembly [23]. Overall, the structure is more relaxed, but still, there exist clear differences between the two local states.

At low temperatures, hard domains are more robust and the size of the domain is relatively large. As a result, more hard waters are found near hard water and vice versa. Figure 8 represents the fraction of hard/soft particles among the nearest neighbors of particles. There is a crossover around 303–323 K and above this temperature, oppositely labeled particles are dominant in the Voronoi neighbors because the size of the domain becomes narrower for the hard domain at higher temperatures. A similar crossover is observed for Voronoi volume and their distributions, too. This leads to a drastic change in RDF, too (Fig. 5(b)). At higher temperatures, the discontinuity in RDFs at first shell is observed. RDF of soft water suddenly drops after the first shell, and the opposite happens for hard water. Since the hard domains are thin and soft domains get very rugged at high temperatures, the interfacial area between two local states increases. Then, the similar-labeled dominant first shell turns to the mixed-labeled second shell.

Around the transient temperature, the skewness changes its sign, too. At low temperatures, hard water distribution has negative skews and soft water distribution has positive skews. But they change their sign above the temperature. The overall number of Voronoi neighbors is larger for soft water. At the interfaces of two domains, their neighbors will have a similar number.

III. CONCLUSION

Our classification shows that ambient water consists of two locally distinct states which are bicontinuously separated. Regardless of the water models, which are different in the way of their dealing with polarizability, we obtain more hard states of water molecules at low temperatures and more soft states of water molecules at high temperatures. The polarization effect may not be very important for the microscopic heterogeneity of water though it may be crucial for specific ion interaction. The fraction of the local states fits with the conventional two-state model.

We also demonstrate that the RDFs of two states reflect their local structural properties. Water molecules in the hard state are more strongly correlated with their neighbors while the spatial correlation of water molecules in the soft state decays very quickly. In fact, their overall features look very similar to those of LDL and HDL. This may suggest that the two local states in ambient water may be emanated from LLCP (Widom Delta). We may check the possibility by examining the same order parameters in the classification of the subcritical state of LLCP. Approaching to LLCP, all particles fall into the soft state of unstructured liquid.

About 303–323 K, the fractions of two states crossover. Above this temperature, the collective mode based on the hydrogen bond network should weaken significantly and the Voronoi volume expands rapidly. It is consistent with the fact that the extrema of the density lie at low temperature. Around this temperature, we find that the domain size of hard particles becomes thin and the interface between hard and soft domains is rugged, which results in oppositely labeled particle prevalence in the second shell of hard particle. As a result, the RDFs becomes discontinuous at the boundary of the first shell and second shell just before the crossover temperature.

In this manuscript, we only focus on the hydrogen bond instigated microscopic heterogeneity. However, this is very difficult to be observed directly in an experiment. In the future, we will connect the microscopic heterogeneity to macroscopic thermodynamic quantities as we have done for gas-liquid critical point [24]. By then, we may move a step closer to understand the origin of the inhomogeneity of water.

ACKNOWLEDGMENTS

This work was supported by Creative Materials Discovery Program through the National Research Foundation of Korea (NRF) funded by Ministry of Science and ICT (NRF-2018M3D1A1058624) and NRF-2018R1A2B6006262.

REFERENCES

[1] C. A. Angell and H. Kanno, Science **193**, 1121 (1976).
[2] A. I. Fisenko and N. P. Malomuzh, Chem. Phys. **345**, 164 (2008).
[3] H. Tanaka, Faraday Discuss. **167**, 9 (2013).
[4] A. Nilsson and L. G. M. Pettersson, Nat. Commun. **6**, 8998 (2015).
[5] P. Gallo *et al.*, Chem. Rev. **116**, 7463 (2016).
[6] L. G. M. Pettersson, R. H. Henchman and A. Nilsson, Chem. Rev. **116**, 7459 (2016).
[7] P. H. Poole, F. Sciortino, U. Essmann and H. E. Stanley, Nature **360**, 324 (1992).
[8] S. Sastry *et al.*, Phys. Rev. E **53**, 6144 (1996).
[9] M. Y. Ha *et al.*, J. Phys. Chem. Lett. **9**, 1743 (2018).
[10] J. L. F. Abascal and C. Vega, J. Chem. Phys. **123**, 234505 (2005).
[11] M. A. González and J. L. F. Abascal, J. Chem. Phys. **135**, 224516 (2011).
[12] G. Lamoureux *et al.*, Chem. Phys. Lett. **418**, 245 (2006).
[13] C. J. Tainter, P. A Pieniazek, Y-S. Lin and J. L. Skinner, J. Chem. Phys. **134**, 184501 (2011).
[14] C. L. Zhao *et al.*, J. Phys. Chem. B **123**, 4594 (2019).
[15] E. D. Cubuk, *et al.*, Phys. Rev. Lett. **114**, 108001 (2015).
[16] S. S. Schoenholz *et al.*, Nat. Phys. **12**, 469 (2016).
[17] P. J. Steinhardt, D. R. Nelson and M. Ronchetti, Phys. Rev. B **28**, 784 (1983).
[18] C. Rycroft, Chaos **4**, 19 (2009).
[19] E. Shiratani and M. Sasai, J. Chem. Phys. **104**, 7671 (1996).
[20] C. C. Chang, C. J. Lin, ACM T. Intel. Syst. Tec. **2**, 27:1 (2011).
[21] A. K. Soper and M. A. Ricci, Phys. Rev. Lett. **84**, 2881 (2000).
[22] V. P. Voloshin and Y. I. Naberukhin, J. Struct. Chem+ **50**, 78 (2009).
[23] D. Chandler, Nature **437**, 640 (2005).
[24] M. Y. Ha *et al.*, arXiv:1902.08360 (2019).